# Using T–Z plots as a graphical method to infer lithological variations from growth strata

Castelltort, Sébastien; Pochat, Stéphane; Van Den Driessche, Jean

**How to cite**

CASTELLTORT, Sébastien, POCHAT, Stéphane, VAN DEN DRIESSCHE, Jean. Using T–Z plots as a graphical method to infer lithological variations from growth strata. In: Journal of structural geology, 2004, vol. 26, n° 8, p. 1425–1432. doi: 10.1016/j.jsg.2004.01.002

This publication URL: https://archive-ouverte.unige.ch/unige:20403
Publication DOI: 10.1016/j.jsg.2004.01.002

ELSEVIER

Journal of Structural Geology 26 (2004) 1425–1432

JOURNAL OF STRUCTURAL GEOLOGY

www.elsevier.com/locate/jsg

# Using T–Z plots as a graphical method to infer lithological variations from growth strata

Sébastien Castelltort*, Stéphane Pochat, Jean Van Den Driessche

*Géosciences Rennes, UMR 6118 du CNRS, Campus de Beaulieu, 35042 Rennes, France*

Received 10 March 2003; received in revised form 22 December 2003; accepted 5 January 2004

Available online 13 February 2004

**Abstract**

The 'T–Z plot' method consists of plotting the throw of sedimentary horizons across a growth fault versus their depth in the hanging wall. This method has been initially developed for the analysis of growth fault kinematics from seismic data. A brief analytical examination of such plots shows that they can also provide valuable information about the evolution of fault topography. When growth is a continuous process, stages of topography creation (fault scarp) and filling (of the space available in the hanging-wall) are related to non-dynamic (draping, mud-prone pelagic settling) and dynamic (sand-prone, dynamically deposited) sedimentation, respectively. In this case, the T–Z plot analysis becomes a powerful tool to predict major lithological variations on seismic profiles in faulted settings.


*Keywords:* Growth fault; Growth strata; Fault-generated topography; Fault kinematics; Net-to-gross ratio

## 1. Introduction

The analysis of syntectonic strata is widely used to infer the kinematics of growth structures (fold and faults) at various degrees of resolution. The graphical method called 'T–Z plot' (Fig. 1) initially developed for the 2D seismic analysis of growth structures consists in plotting, for each horizon, the stratigraphic throw T of the considered marker versus its depth Z (Tearpock and Bischke, 1991; Bischke, 1994).

This method can be used to constrain the slip history of growth faults by assuming a "fill-to-the-top" sedimentation, i.e. sedimentation always fills-up fault-generated topography (e.g. Mansfield and Cartwright, 1996; Cartwright et al., 1998).

However, several studies have documented sedimentation disturbances induced by fold- and fault topographies on the sea floor, and show that fault scarps can induce, for example, deviation or reflection of sedimentary flows, localized erosion, or by-pass phenomena (e.g. Bornhauser, 1959; Edwards, 1976; Thornburg et al., 1990; Ravnas and Steel, 1997; Morris et al., 1998; Soreghan et al., 1999; Anderson et al., 2000; Hodgetts et al., 2001; Hooper et al., 2002; Shaw et al., 2003). This means that fault-generated topographies occur at the depositional surface, and that the fill-to-the-top assumption may not always be valid.

This paper studies the significance of T–Z plots for two end-members: (1) a fill-to-the-top sedimentation with variable slip rate, and (2) a more general model that combines variable displacement and occurrence of topography.

The implications of both end-members are examined and lead us to propose T–Z plots as a graphical tool to infer the lithology of growth strata from subsurface data.

## 2. Construction and interpretation of T–Z plots

Let us consider the case of a normal growth fault in which $n$ stratigraphic horizons can be correlated across the fault (Fig. 2A). In the following, the younger horizon at $i = 0$ is the first stratigraphic surface without fault-generated topography across the fault, and the older $i = n$ is the youngest pre-faulting horizon (Fig. 2A). If palaeobathymetry and the age of each horizon are known, fault slip rates and topography evolution are known directly. However, in the absence of such information, which is

* Corresponding author. Now at: Department of Earth Sciences, ETH-Zentrum, Sonneggstrasse 5, CH-8092 Zürich, Switzerland. Tel.: +41-1-632-3676; fax: +41-1-632-1080.

*E-mail address:* sebastien.castelltort@erdw.ethz.ch (S. Castelltort).

0191-8141/$ - see front matter © 2004 Elsevier Ltd. All rights reserved.
doi:10.1016/j.jsg.2004.01.002

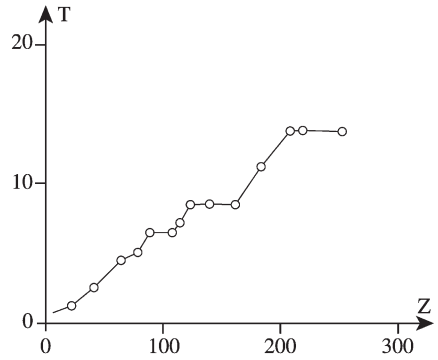


Fig. 1. Example of throw (T, vertical axis) versus depth (Z, horizontal axis) plot constructed from high-resolution seismics across a growth fault in the Gulf coast sediments, offshore Texas, late Pleistocene to recent (modified after Cartwright et al., 1998). Values are in metres. In their work, assuming fill-to-the-top sedimentation, Cartwright et al. (1998) show that positive slopes represent growth phases and horizontal portions represent phases of fault inactivity.

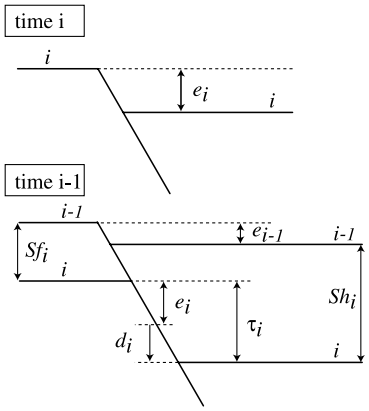


Fig. 3. General relationships between vertical throw ($\tau_i$), displacement ($d_i$), stratigraphic thicknesses ($Sh_i$ and $Sf_i$) and fault topography ($e_i$ and $e_{i-1}$) during one step of fault growth.

generally the case, only the thickness of growth strata may provide information about fault kinematics.

The construction of the corresponding T–Z plot (Fig. 2B) consists of plotting the vertical throw $T_i$ of each horizon versus the associated depth $Z_i$ in the hanging-wall.

The problem is to interpret the slope variations that occur on the T–Z plot.

In the general case, the throw contains the displacement and the pre-existing topography (Fig. 3). Therefore, the expression of the throw $\tau_i$ on the first increment of deposition (interval $[i; i-1]$) after time $i$ (Fig. 3) is:

$$\tau_i = d_i + e_i \tag{1}$$

where $d_i$ is the vertical displacement on the fault between $i$ and $i-1$, and $e_i$ is the topography at time $i$ (Fig. 3). All the subsequent increase in throw is due to the displacement on the fault, and the expression of the total throw $T_i$ of horizon $i$ at instant 0 is:

$$T_i = \sum_{i}^{0} d_i + e_i \tag{2}$$

where $\sum_i^0 d_i$ represents the displacement due to fault growth from time $i$ up to the end of fault activity (time 0).

If no data on paleotopography at each instant is available, two end-members models may be considered: (1) the 'fill-to-the-top' model, and (2) the variable displacement/topography model.

### 2.1. The fill-to-the-top model

In some cases, the sedimentation can be considered as filling-up fault-generated topography, which is known as the 'fill-to-the-top model' (e.g. Gawthorpe et al., 2000; Masaferro et al., 2002). In such cases, the topography at each instant is zero ($e_i = 0 \forall i$, cf. Fig. 4). Therefore, removing topography from Eq. (2) gives the expression of the final throw and throw variations in the fill-to-the-top model, where $Sh_i$ and $Sf_i$ are the thickness of sediments

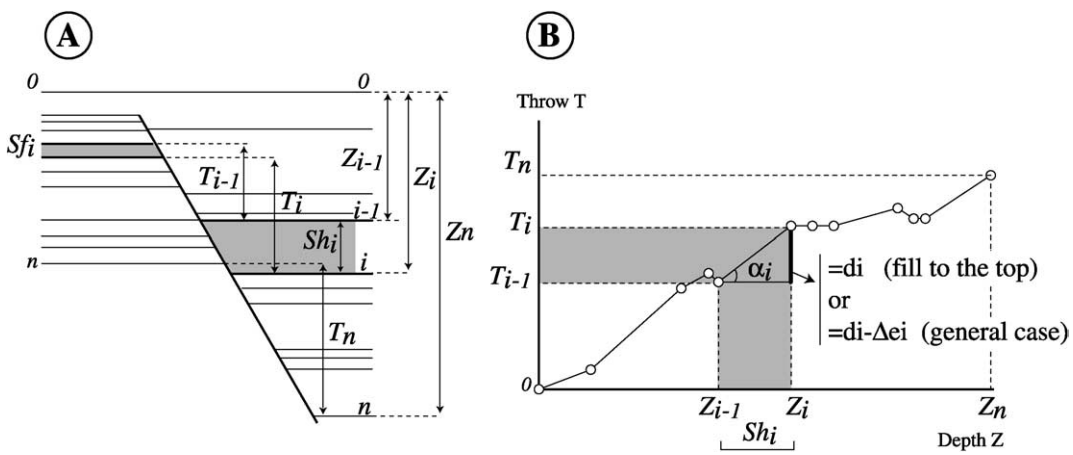


Fig. 2. Principle of T–Z plot construction. (A) Example of correlated stratigraphic markers across a normal growth fault. (B) Corresponding T–Z plot.

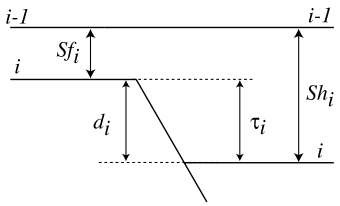


Fig. 4. Relationships between stratigraphic thicknesses, throw and displacement in the 'fill-to-the-top' case.

deposited between $i$ and $i-1$ in the hanging-wall and on the footwall, respectively (Fig. 4):

$$\tau_i = d_i = Sh_i - Sf_i \tag{3}$$

$$T_i = \sum_{i}^{0} d_i \tag{4}$$

$$T_i - T_{i-1} = \sum_{i}^{0} d_i - \sum_{i-1}^{0} d_i = d_i \tag{5}$$

The slope $\alpha_i$ of the T–Z plot on each interval (Fig. 2B) is then given by:

$$\alpha_i = \frac{T_i - T_{i-1}}{Z_i - Z_{i-1}} = \frac{d_i}{Sh_i} \tag{6}$$

As long as time is not known and only layer thicknesses are available, the slope of the T–Z plot only indicates the slip rate relative to the sedimentation rate on each interval:

$$\alpha_i = \frac{d_i/t_i}{Sh_i/t_i} \tag{7}$$

where $t_i$ is the duration of interval $[i; i-1]$. In other words, even if the sedimentation rate exceeds the vertical component of displacement (i.e. fill-to-the-top model), the slope variations on the T–Z plot cannot be linked in a straightforward way to fault activity. For example, Eq. (7) shows that with a constant displacement rate, variations in the sedimentation rate only will induce slope variations on the T–Z plot.

Therefore, while throw variations give the absolute magnitude of vertical displacement (Fig. 2B) and can be interpreted as such, the slope variations should be interpreted carefully, unless time is known, by taking into consideration the variations of thickness.

The slope can be expressed in terms of strata thickness variation by substituting Eq. (3) into Eq. (6):

$$\alpha_i = \frac{Sh_i - Sf_i}{Sh_i} = 1 - EI^{-1} \tag{8}$$

where $EI = Sh_i/Sf_i$ is the expansion index as defined by Thorsen (1963).

In this way, the additional information displayed by T–Z plots, which lacks in the expansion index method of Thorsen (1963), is the absolute magnitude of vertical displacement on fault (Cartwright et al., 1998).

However, intervals of zero slope (i.e. intervals with no throw variation) necessarily indicate periods of fault inactivity in the fill-to-the-top model, i.e. expansion index of 1. This has been used, for example, in the analysis of a set of normal growth faults from the Gulf of Mexico to put forward their polycyclic activity (Cartwright et al., 1998).

Similarly a negative slope would imply a negative displacement, i.e. an inversion of the fault. In an alternative explanation, Mansfield and Cartwright (1996) proposed that a negative slope might be associated with overlap and linkage processes due to fault propagation.

### 2.2. The variable displacement/topography model

As mentioned above, several studies have indicated the presence of fault- or fold-generated topography in currently active settings and for fossilized growth structures. In addition, it is known that pelagic sedimentation can drape topography with equivalent sediment thicknesses on both the hanging wall and the footwall (Cartwright et al., 1998). In such cases, the topography $e_i$ at each time can be different from zero (Fig. 3), and cannot be further neglected. It follows that throw variations represent a combination of displacement and topography as shown by Eq. (2).

We propose here to conciliate both the fill-to-the-top model and the occurrence of fault-generated topographies.

The general expression of slope on any interval $[i; i-1]$ from Eq. (1) is:

$$\alpha_i = \frac{T_i - T_{i-1}}{Sh_i} = \frac{\left(\sum_{n=i}^{n=0} d_n - e_i\right) - \left(\sum_{n=i-1}^{n=0} d_n - e_{i-1}\right)}{Sh_i} \tag{9}$$

which can be written as:

$$\alpha_i = \frac{d_i - \Delta e_i}{Sh_i} \tag{10}$$

where $\Delta e_i$ is the variation of topography between $i$ and $i-1$ (i.e. $\Delta e_i = e_i - e_{i-1}$) (Fig. 2A and B). For a constant displacement $d_i$, the slope increases when topography diminishes from $i$ to $i-1$. As a consequence, on a T–Z plot, the points $[T_i; Z_i]$, which follow the stronger slopes may be interpreted with confidence as representing low to zero topography. By contrast, between two such points, the other points follow lower or even negative slopes and result from the creation of topography. Moreover, the first ($i = 0$) and the last ($i = n$) points of the T–Z plots do not record any topography. Indeed, there is no reason that a topography exists before faulting ($i = n$). The last horizon ($i = 0$) is a horizontal marker by definition.

Therefore, on any T–Z plot, the $m$ portion between the points of assumed low topography can be drawn, starting from $j = 0$, at the origin of the T–Z plot, to $j = m$(for the

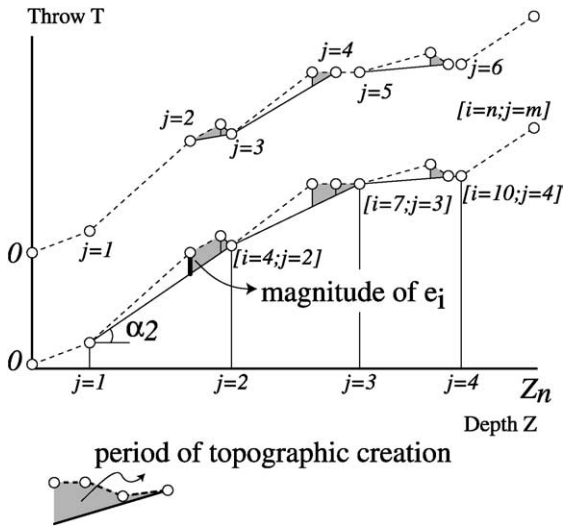


Fig. 5. T–Z plot interpretation of the fault of Fig. 2A in the case of variable displacement/topography model. The portions represent intervals of constant displacement (with $\alpha_j$ the mean displacement rate), and the shadowed areas denote periods of topography creation. The upper and lower two curves represent different choices of portions, which involve different topography magnitudes (see text).

older horizon) (Fig. 5). The slope of each of these portions represents the mean displacement rate relative to the sedimentation rate on the considered interval, and the deviations of the T–Z curve with respect to these portions represent creation of fault-generated topography (shadowed areas on Fig. 5). In this way, a fill-to-the-top sedimentation is implicitly assumed to work at the resolution of the chosen portions and topographies occur at a higher frequency due to sedimentation changes. The only condition to respect when choosing intervals of steady growth is that there should be no point $[T_i; Z_i]$ of any interval $[j; j-1]$ situated below the corresponding portion $j$ on the diagram. Indeed, such a situation would imply a negative topography at time of deposition of horizon $i$ (i.e. horizon $i$ topographically higher in the hanging wall than on the footwall), which would be unlikely.

The expression of the throw $T_i$ of each horizon $i$ in any interval $[j; j-1]$ becomes:

$$T_i = T_{j-1} + \frac{T_j - T_{j-1}}{Z_j - Z_{j-1}}\left(Z_i - Z_{j-1}\right) + e_i \tag{11}$$

$$T_i = T_{j-1} + \alpha_j\left(Z_i - Z_{j-1}\right) + e_i \tag{12}$$

where $\alpha_j$ is the slope of the portion $j$, and represents the mean displacement rate (relative to the mean sedimentation rate) on this interval. With this method, the T–Z contains the magnitude of the displacement on the fault at the portion resolution (intervals of $j$), and the evolution of topography at each instant $i$ by the deviation of the curve from the portions. Choice of the number of those portions of the T–Z plot should be made as the scale at which slope variations on the T–Z plot can no longer be associated with lithological changes on well log data. The T–Z plot used in this way provides the relative evolution of the topography on the fault which is possibly linked to sedimentation evolution.

## 3. Discussion

Fill-to-the-top and variable displacement/topography models lead to fundamentally different interpretations. In the fill-to-the-top model, the slope variations on a T–Z plot are associated with displacement variations on the fault. Therefore, in the fill-to-the-top model, there is a priori neither lithological nor sediment flux variations, which implies that sedimentation be always dynamic. On the contrary, in the variable displacement/topography model, the slope variations are interpreted as topography creation or filling linked to sediment flux variations superimposed on a constant displacement signal over given time steps. These sediment flux variations may be linked to changes in sedimentation dynamics and lithology. For example, pelagic type sedimentation will leave equivalent thicknesses across a fault and therefore induce the creation of a topography during fault activity. Inversely, dynamic sedimentation (sands) will more likely tend to fill fault-generated topographies.

An obvious way to choose between the two models is to compare T–Z plots with sedimentary well logs data. If no major lithological variation is observed, then T–Z slope variations are rather related to variable fault activity. However, if slope variations can be correlated with lithological variations, then the T–Z plot may indicate sedimentation changes.

We have reported elsewhere in detail (Pochat et al., 2004) an application of this method to a growth fault located in the Niger delta and which affects Oligocene to early Miocene deltaic series. The T–Z plot drawn from the line drawing of a seismic section across this fault (Fig. 6A) shows marked alternations between positive and zero slope portions (Fig. 6B). Based on biostratigraphic constraints (Pochat, 2003), the studied series have been found to be comprised between 29.8 and 18 Ma. Following the theoretical study developed in the present work, two different interpretations of these high-frequency alternations are possible: (1) in the case of a fill-to-the-top sedimentation, those alternations may represent alternations between phases of fault growth and inactivity, respectively, and (2) if displacement on the fault is assumed as constant, then those alternations may represent an alternation of phases of creation and filling of the fault-generated topography by sedimentary processes alternatively non-dynamic and dynamic, respectively.

In order to test this latter hypothesis, we have drawn a synthetic lithological column by attributing a shale lithology to each zero slope portion of the T–Z plot, and a sand lithology to each positive slope portion (Fig. 7). Comparison of this synthetic lithological column with borehole lithogical data in the hanging wall shows a good correspondence

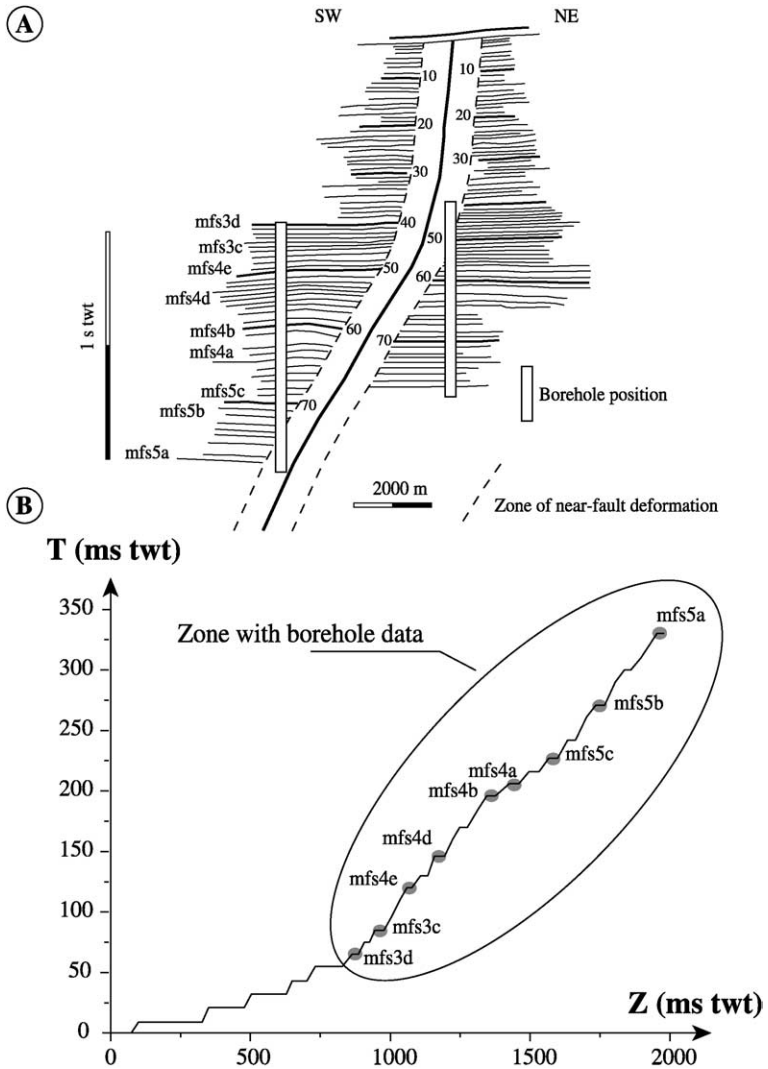


Fig. 6. Case study in the late Oligocene to early Miocene Niger delta deposits (modified after Pochat et al., 2004). (A) Line drawing of a seismic section (in twt) crossing the studied fault and showing the horizons used in the construction of the T–Z plot, the position of the maximum flooding surfaces, and the localization of the borehole data. The throw and depth relationships of those horizons have been taken away from the delineated zone of near-fault deformation to avoid artefacts in the T–Z plot. (B) Corresponding T–Z plot (in twt) with the zone covered by borehole data (circled), and the position of the mfs (shadowed).

between shaly intervals identified on the T–Z plot and shaly intervals documented on the borehole data (Fig. 7). In particular, all the shales linked to maximum flooding surfaces (mfs3d–mfs5a) have been correctly found with the T–Z plot method. Other shaly intervals (numbered 1–6 on Fig. 7) found between the maximum flooding surfaces on the T–Z plot can also be correlated with shales on the well log data. However a number of shaly intervals on the borehole do not find correspondence on the synthetic column. This may be mainly due to the lower resolution of the seismic data (and thus of the T–Z plot) compared with well log resolution (Pochat et al., 2004).

The sand/shale ratios (net-to-gross ratios) obtained from the T–Z analysis and those shown by the borehole data are very close, at the scale of the whole series (60/40 on the synthetic column and 55/45 on well log) as at the scale of the regressive–transgressive cycles (R–T cycles C1–C8 on Fig. 7) with a maximum misfit of 15%. Except for cycles C5 and C6, where a large shale-body has not been predicted by the T–Z analysis, the net-to-gross ratios differ significantly between the synthetic and the real columns. The reasons for this have been discussed elsewhere but may basically be explained in two ways: (1) this shale body was initially present on the footwall but subsequently eroded, producing an excess thickening of this body in the hanging wall, and therefore appearing as a sandy (thickened) unit through the T–Z method, i.e. represented with positive slope on the T–Z plot, or (2) if this body represents a more than 100 ka period of deposition, it could have diffused from the footwall to the hanging wall, by creeping down (Mitchell, 1996) and/or redistribution of particles by bottom currents, wave or tidal action, thus inducing a thickening of this body in the hanging wall.

This example shows that the T–Z plot method works

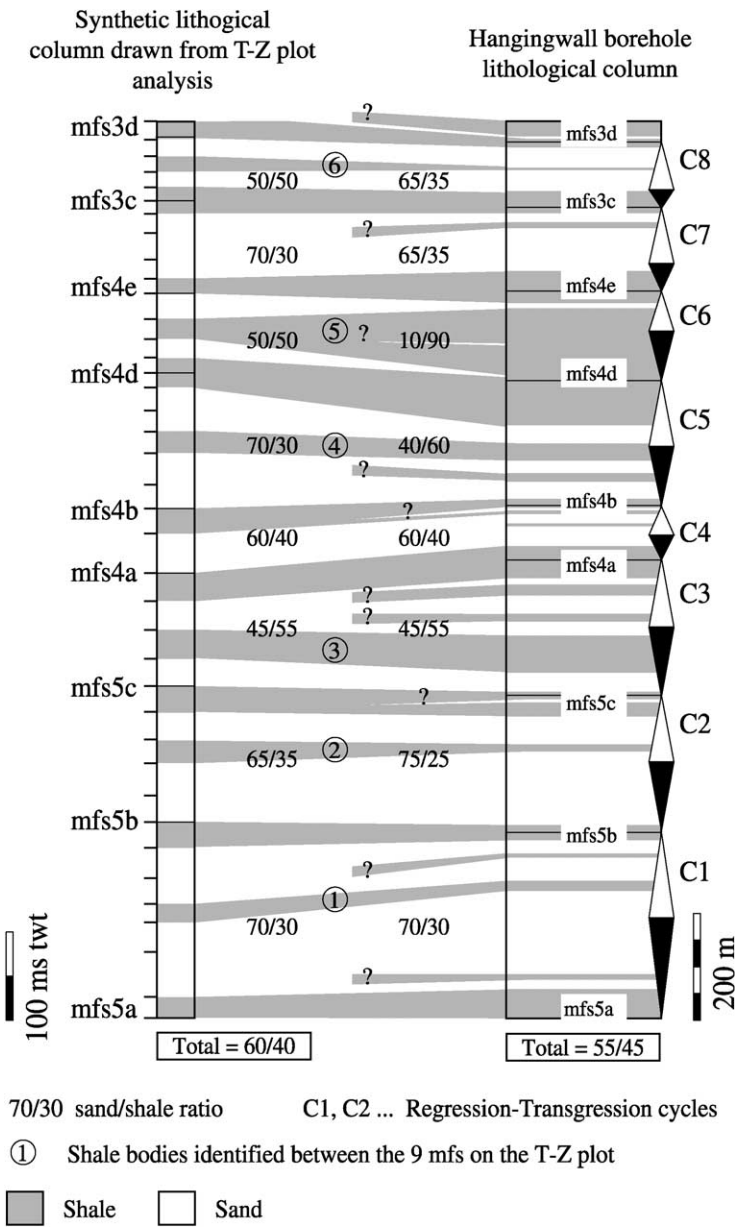


Fig. 7. Comparison of the synthetic lithological column drawn from the T–Z plot analysis with the borehole data in the hanging wall. The synthetic column has been constructed assuming that zero slope intervals of the T–Z plot represent periods of non-dynamic sedimentation, linked to shale deposition, and positive slope intervals represent periods of dynamic sedimentation attributed to sands. The comparison shows a good correspondence between shale intervals predicted by the T–Z plot analysis and the shale intervals found on borehole data.

satisfactorily to predict sand–shale alternations from the seismic analysis of growth faults. This also puts forward that the studied fault may have had an almost continuous activity at this scale, and extends to higher frequencies (<1 Ma) the previous finding that faults can have a continuous behaviour over several million years (Nicol et al., 1997). However, the method still needs to be further tested, and our results do not preclude the existence of high-frequency polycyclic motion on growth faults as evidenced elsewhere (e.g. Cartwright et al., 1998).

A remark should be added regarding the effects of compaction. In such settings where we expect to find sand–shale alternations, differential compaction may produce thickness variations between the two fault compartments that may not express the initial depositional thickness relationships. If the fault has a large throw compared with the total sedimentary thickness, this differential compaction cannot be neglected (Hegarty et al., 1988; Forbes et al., 1991). For example, with 1000 m of throw, sedimentary layers on the footwall of a growth fault may be 20% less compacted than the same layers in the hanging wall (Forbes et al., 1991). Therefore, sediments in the hanging wall may be over-compacted compared with the footwall. This is valid for both sand- and mud-prone sediments, but should be

stronger for mud-prone sediments. This will tend to diminish the slopes on the T–Z plot, and to diminish them in excess for mud-prone sediments, which will enhance the effects outlined in the present work, i.e. slope diminutions may indicate mud-prone sediments. Also, when alternances of positive and zero slope portions are observed on a T–Z plot, it seems unlikely that this can be an artefact due to compaction. Indeed, it is highly unlikely that compaction acts in such a way that each layer of shale in the hanging wall be exactly compacted by the amount necessary to get the same thickness as on its footwall counterpart. And even if this were the case, this would again help in finding the shaly intervals.

Attention should also be paid to the 3D aspects of this problem. The sediment pathways and environments can vary strongly spatially and temporally in relation to fold and fault population evolution (e.g. Gawthorpe and Leeder, 2000; Young et al., 2002). For example, erosion can occur in the hanging wall of the normal faults due to deviation of currents by fault topography. Such 3D processes will affect the topography at the fault emergence, which will be reflected on the T–Z plot. To decipher between the possible causes for slope changes on the T–Z plot and thus topographic evolution of the fault, it will therefore be necessary to compare the T–Z plots with data on sedimentology and stratigraphy where available. Also, a distinction can be made between 3D effects (related in some way to local fault geometry), which may have only a local signature, and more regionally extensive sedimentary events, e.g. allogenic basin-scale sedimentation changes (maximum flooding surfaces, systems tracts). Using the T–Z method in a particular case implies taking into account the local and regional basin factors related to that particular setting (sedimentology, stratigraphy and structural geology).

## 4. Conclusion

The T–Z plot method can be proposed as a simple additional tool to aid in the prediction of growth strata lithologies and the correlation of sand–shale successions (net-to-gross ratio) inside a basin and across growth structures where well log data are not available everywhere. Slope variations on a T–Z plot may be quantitatively altered by the 3D evolution of fault growth and related depositional patterns evolution, as well as by compaction effects. However, most important is the qualitative evolution of slopes on the T–Z plots, and such effects can be easily ruled out when compared with real well data if available, or based on their spatial robustness. Well correlatable slope changes between several T–Z plots inside a basin can be viewed as robust features, and possible regional or local sedimentation changes.

## Acknowledgements

This research was partially aided by TotalFinaElf, which funded Stephane Pochat's PhD and provided him material to apply the method. Reviews by Mike Young and an anonymous reviewer greatly improved the clarity and organization of the manuscript. We acknowledge Joe Cartwright and John J. Walsh for their early comments on some ideas involved in this work. Warm thanks to our friends C. Glumeux, K. Bernard, Bobby Loget, J. Pabo, C. Agada, M. Gautier, V. Blez, R. Bourboullec, F. Caña, A. Pitra, Angus Young and others for their support during a wet stage in Rennes.

## References

Anderson, J.E., Cartwright, J., Drysdall, S.J., Vivian, N., 2000. Controls on turbidite sand deposition during gravity-driven extension of a passive margin: examples from Miocene sediments in Block 4, Angola. Marine and Petroleum Geology 17, 1165–1203.

Bischke, R.E., 1994. Interpreting sedimentary growth structures from well log and seismic data (with examples). American Association of Petroleum Geologists Bulletin 78 (6), 873–892.

Bornhauser, M., 1959. Depositional and structural history of Northwest Hartburg Field, Newton County, Texas. American Association of Petroleum Geologists Bulletin 44 (4), 458–470.

Cartwright, J., Bouroullec, R., James, D., Johnson, H., 1998. Polycyclic motion history of some Gulf Coast growth faults from high-resolution displacement analysis. Geology 26 (9), 819–822.

Edwards, M.B., 1976. Growth faults in Upper Triassic deltaic sediments. American Association of Petroleum Geologists Bulletin 60 (3), 341–355.

Forbes, P.L., Ungerer, P.M., Kuhfuss, A.B., Riis, F., Eggens, S., 1991. Compositional modeling of petroleum generation and expulsion; trial application to a local mass balance in the Smorbukk Sor Field, Haltenbanken area, Norway. American Association of Petroleum Geologists Bulletin 75 (5), 873–893.

Gawthorpe, R.L., Leeder, M.R., 2000. Tectono-sedimentary evolution of active extensional basins. Basin Research 12 (3–4), 195–218.

Gawthorpe, R.L., Hall, M., Sharp, I., Dreyer, T., 2000. Tectonically enhanced forced regressions: examples from growth folds in extensional and compressional settings, the Miocene of the Suez rift and the Eocene of the Pyrenees. In: Hunt, D., Gawthorpe, R.L. (Eds.), Sedimentary Responses to Forced Regressions. Geological Society (London) Special Publications 172, pp. 177–191.

Hegarty, K.A., Weissel, J.K., Mutter, J.C., 1988. Subsidence history of Australia's southern margin: constraints on basin models. American Association of Petroleum Geologist Bulletin 72 (5), 615–633.

Hodgetts, D., Imber, J., Childs, C., Flint, S., Howell, J., Kavanagh, J., Nell, P., Walsh, J., 2001. Sequence stratigraphic responses to shoreline-perpendicualr growth faulting in shallow marine reservoirs of the Champion field, offshore Brunei Darussalam, South China Sea. American Association of Petroleum Geologists Bulletin 85 (3), 433–457.

Hooper, J.R., Fitzsimmons, R.J., Grant, N., Vendeville, B.C., 2002. The role of deformation in controlling depositional patterns in the south-central Niger Delta, West Africa. Journal of Structural Geology 24, 847–859.

Mansfield, C.S., Cartwright, J.A., 1996. High resolution displacement mapping from 3-D seismic data. Journal of Structural Geology 18, 249–263.

Masaferro, J.L., Bulnes, M., Poblet, J., Eberli, G.P., 2002. Episodic folding

inferred from syntectonic carbonate sedimentation: the Santaren anticline, Bahamas foreland. Sedimentary Geology 146, 11–24.

Mitchell, N.C., 1996. Creep in pelagic sediments and potential for morphological dating of marine fault scarps. Geophysical Research Letters 23, 483–486.

Morris, S.A., Alexander, J., Kenyon, N.H., Limonov, A.F., 1998. Turbidites around an active fault scarp on the Lower Valencia Fan, northwest Mediterranean. Geo-Marine Letters 18, 165–171.

Nicol, A., Walsh, J.J., Watterson, J., Underhill, J.R., 1997. Displacement rates of normal faults. Nature 390, 157–159.

Pochat, S., 2003. Escarpement de faille synsédimentaire: perturbation des écoulements gravitaires sous-marins et détermination de la cinématique des failles. Ph.D. thesis, University of Rennes, Mémoires de Géosciences Rennes 106pp.

Pochat, S., Castelltort, S., Van Den Driessche, J., Besnard, K., Gumiaux, C., 2004. A simple method to determine sand–shale ratios from the seismic analysis of growth faults. Example from late Oligocene to early Miocene Niger delta deposits. American Association of Petroleum Geologists Bulletin, submitted.

Ravnas, R., Steel, R.J., 1997. Contrasting styles of Late Jurassic syn-rift turbidite sedimentation: a comparative study of the Magnus and Oseberg areas, northern North Sea. Marine and Petroleum Geology 14 (4), 417–449.

Shaw, J.H., Novoa, E., Connors, C.D., 2003. Structural controls on growth stratigraphy. In: McClay, K., (Ed.), Thrust Tectonics and Petroleum Systems, American Association of Petroleum Geologists Memoir, in press.

Soreghan, M.J., Scholz, C.A., Wells, J.T., 1999. Coarse-grained, deep-water sedimentation along a border fault margin of Lake Malawi, Africa: seismic stratigraphic analysis. Journal of Sedimentary Research 69, 832–846.

Tearpock, D., Bischke, R.E., 1991. Applied Subsurface Geological Mapping. Prentice-Hall, New York.

Thornburg, T.M., Kulm, L.D., Hussong, D.M., 1990. Submarine-fan development in the southern Chile Trench: a dynamic interplay of tectonics and sedimentation. Geological Society of America Bulletin 102, 1658–1680.

Thorsen, C.E., 1963. Age of growth faulting in Southeast Louisiana. Transactions Gulf Coast Association of Geological Societies 13, 103–110.

Young, M.J., Gawthorpe, R.L., Sharp, I.A., 2002. Architecture and evolution of syn-rift clastic depositional systems towards the tip of a major fault segment, Suez Rift, Egypt. Basin Research 14 (1), 1–23.